

Impact of hydrogen on indium incorporation at m -plane and c -plane $\text{In}_{0.25}\text{Ga}_{0.75}\text{N}$ surfaces: First-principles calculations

John E. Northrup

Palo Alto Research Center, 3333 Coyote Hill Road, Palo Alto, California 94304, USA

(Received 31 October 2008; revised manuscript received 9 December 2008; published 27 January 2009)

We present first-principles calculations for m -plane and c -plane $\text{In}_{0.25}\text{Ga}_{0.75}\text{N}$ surfaces. The results elucidate the dependence of indium incorporation on growth conditions. For both surfaces the calculations indicate that In incorporation is energetically favorable provided the surface is wetted by In adlayers rather than passivated by hydrogen and NH_2 groups. Growth of an $\text{In}_{0.25}\text{Ga}_{0.75}\text{N}$ alloy therefore requires that the chemical potential of hydrogen be kept low. The results predict that a reduction in the abundance of hydrogen can lead to greater In incorporation on the m plane as well as the c plane.

DOI: [10.1103/PhysRevB.79.041306](https://doi.org/10.1103/PhysRevB.79.041306)

PACS number(s): 68.35.Md, 68.35.B-, 81.30.Bx

There is substantial interest in developing powerful and compact lasers having emission wavelengths of approximately 500 nm. A promising approach to achieving this goal is to employ the $\text{In}_x\text{Ga}_{1-x}\text{N}$ alloy system with an In composition of approximately 25% in the active region in order to achieve the appropriate band gap.¹ However, growth of quantum wells with high In content is challenging for a variety of reasons, including phase separation and formation of extended defects.^{2,3} The large size mismatch between In and Ga (InN bonds are $\sim 11\%$ longer than GaN bonds) and the relative weakness of the InN bond are the primary causes of the instabilities.^{4,5} The problematic nature of InGaN growth, along with the issue of polarization fields, has led to studies of InGaN growth on a range of surface orientations.⁵⁻¹⁷ In this work we explore the growth conditions needed for achieving high levels of indium incorporation on the m plane and c plane.

Experimental studies of InGaN growth on c -plane nitrides observed that a reduction in the H_2 flow leads to an increase in the amount of indium that is incorporated.^{16,17} The origin of this effect is not understood. On the basis of first-principles pseudopotential density-functional calculations, we propose that this effect arises from variations in surface structure driven by changes in the chemical potential of hydrogen. We analyze surface reconstructions having various indium compositions and determine the stability of the structures as a function of the chemical potentials of hydrogen and indium. The primary result is that an adlayer of In stabilizes In incorporation in group-III sites just below the adlayer. In contrast, if the surface is passivated by H and NH_2 groups the incorporation of In at the surface is not favorable. The results predict that a reduction in the abundance of hydrogen can lead to more In incorporation on the m plane as well as the c plane.

The investigation of the surface thermodynamics is based on density-functional theory (DFT). Chemical potentials are introduced to enable comparisons of relative stability of surfaces with different quantities of In, Ga, N, and H, such as they might occur under metal-organic chemical-vapor-deposition conditions (MOCVD). A formalism which includes the vibrational contributions to the free energy arising from adsorbed H is employed.¹⁸⁻²⁰ We consider structurally relaxed InGaN surfaces having in-plane lattice constants cor-

responding to an indium concentration of 25%. Previous theoretical investigations of indium incorporation at the surface considered hydrogen-free GaN(0001) surfaces having the bulk in-plane lattice constant.^{14,15}

Because the growth of an $\text{In}_{0.25}\text{Ga}_{0.75}\text{N}$ alloy necessitates extremely N-rich conditions, the chemical potential of nitrogen (μ_{N}) is taken to be very high: $\mu_{\text{N}} = \frac{1}{2}E(\text{N}_2)$, where E is the energy of a N_2 molecule. In addition we assume equilibrium with an $\text{In}_{0.25}\text{Ga}_{0.75}\text{N}$ compound, which allows us to write $0.25\mu_{\text{In}} + 0.75\mu_{\text{Ga}} + \mu_{\text{N}} = E(\text{In}_{0.25}\text{Ga}_{0.75}\text{N})$.²¹ These two conditions are employed to eliminate the N and Ga chemical potentials as variables. The chemical potentials of indium (μ_{In}) and hydrogen (μ_{H}) are then treated as the independent variables and allowed to vary within physically relevant ranges. The upper limit on μ_{In} is the energy per atom of bulk indium. The hydrogen chemical potential can be related to the temperature and partial pressure (p_{H}) of hydrogen.¹⁸ The chemical potential of hydrogen may be reduced by lowering the partial pressure of the H_2 carrier gas. The indium chemical potential may be controlled by tuning the flow rate of the trimethylindium source gas.

Total energies and atomic positions are determined by first-principles pseudopotential-DFT calculations that employ the local-density approximation.²²⁻²⁶ The plane-wave cut-off energy for the solutions to the Kohn-Sham equations is $E_{\text{cut}} = 60$ Ry. Troullier and Martins pseudopotentials are employed for In, Ga, and N, and the Ga $3d$ and In $4d$ electrons are included as valence states. For hydrogen the exact $1/r$ potential is employed. This approach is similar to that employed in previous studies.^{14,15,18,20}

For the $(10\bar{1}0)$ surfaces a supercell having 1×2 translational symmetry is employed with perpendicular lattice vectors $\mathbf{e}_1 = \mathbf{c}$, and $\mathbf{e}_2 = 2\mathbf{a}$. The lengths of \mathbf{c} and \mathbf{a} are determined by energy minimization for a bulk $\text{In}_{0.25}\text{Ga}_{0.75}\text{N}$ compound and have values of 5.34 and 3.27 Å, respectively. These lattice constants are expanded by a factor of 1.03 in comparison to those corresponding to bulk GaN. For the (0001) surfaces a 2×2 cell is employed, and the hexagonal lattice constant has length $|2\mathbf{a}| = 6.54$ Å. The sampling of the Brillouin zone employs a $4 \times 4 \times 1$ grid of \mathbf{k} -points for both surfaces. The cells employed contain five double layers.

The phase diagram for the m -plane surface is shown in Fig. 1. The diagram is determined by finding which structure

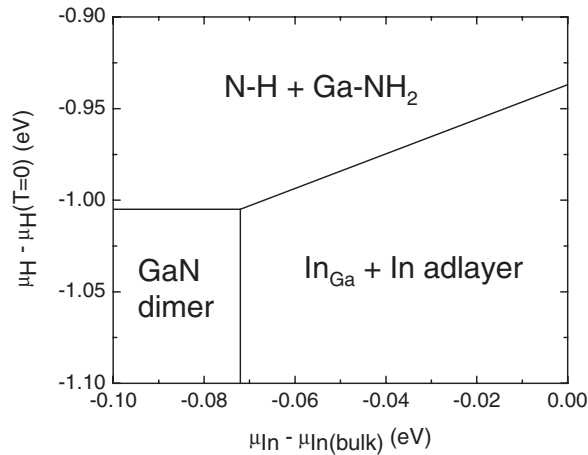


FIG. 1. Results are shown for the m -plane. $T_{\text{growth}}=700$ °C. This plot indicates the lowest-energy surface structure for various values of the H and In chemical potentials. Indium can be incorporated at the surface in group-III sites in the $\text{In}_{\text{Ga}}+\text{In}$ adlayer structure, which is stable in the lower right region. In both the Ga-N dimer structure and the $\text{N-H}+\text{Ga-NH}_2$ structure In_{Ga} formation is not energetically favorable. The H chemical potential is referenced to the energy/atom of an H_2 molecule at $T=0$. The indium chemical potential is limited by the onset of bulk indium condensation.

minimizes the formation energy for a given pair (indium and hydrogen) of chemical potentials. The boundary lines separating different regions correspond to chemical potentials for which the two structures have the same formation energy. Depending on the values of μ_{H} and μ_{In} , three different structures are stable. These structures are illustrated in Fig. 2. In the lower left region of Fig. 1 (low μ_{H} and low μ_{In}) the Ga-N dimer surface shown in Fig. 2(a) is stable. In the lower right part of the diagram (low μ_{H} and high μ_{In}) the $\text{In}_{\text{Ga}}+\text{In}$ adlayer structure shown in Fig. 2(f) is stable, and in the upper part of the diagram (high μ_{H}) the $\text{N-H}+\text{Ga-NH}_2$ surface shown in Fig. 2(c) is stable.

The calculations indicate that the indium adlayer structure facilitates the incorporation of indium. In contrast, the Ga-N dimer and the $\text{N-H}+\text{Ga-NH}_2$ surfaces are not conducive to indium incorporation. When an indium adlayer wets the surface it is energetically favorable to incorporate indium. This is seen by comparing the energy of the In adlayer structure shown in Fig. 2(e) with the $\text{In}_{\text{Ga}}+\text{In}$ adlayer structure shown in Fig. 2(f). Replacing the Ga atom by an In atom lowers the energy by 0.24 eV/atom for $\mu_{\text{In}}=\mu_{\text{In}(\text{bulk})}$. An indium atom occupying such a site will likely be buried in the subsequent overgrowth by the next layer and permanently incorporated into the bulk.

As illustrated in Fig. 1, the stability of the In adlayer and the concomitant indium incorporation require that the hydrogen chemical potential be low. In the In-rich limit the requirement to stabilize the $\text{In}_{\text{Ga}}+\text{In}$ adlayer structure is $\mu_{\text{H}} < \mu_{\text{H}}(T=0) - 0.93$ eV. If the hydrogen chemical potential exceeds this value, then the N and Ga atoms at the surface become saturated by H and NH_2 groups, and In incorporation is inhibited. In the region where the $\text{N-H}+\text{Ga-NH}_2$ surface is stable it costs energy to replace the Ga by In. The minimum energy cost to create the $\text{In}_{\text{Ga}}+\text{N-H}+\text{Ga-NH}_2$ structure,

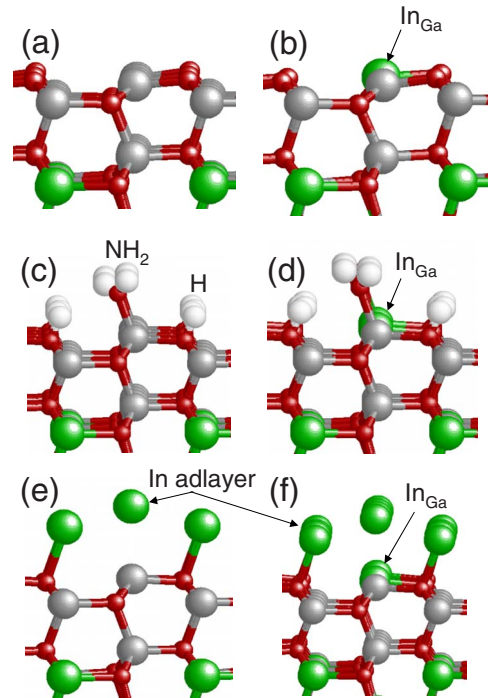


FIG. 2. (Color online) Possible reconstructions of the InGaN m -plane surface are shown. (a) Ga-N dimer. (b) $\text{In}_{\text{Ga}}+\text{Ga-N}$ dimer. (c) $\text{N-H}+\text{Ga-NH}_2$. (d) $\text{In}_{\text{Ga}}+\text{N-H}+\text{Ga-NH}_2$. (e) In adlayer. (f) $\text{In}_{\text{Ga}}+\text{In}$ adlayer. In atoms are large green/light gray spheres, Ga atoms are gray, N atoms are small red/gray spheres, and H atoms are white.

shown in Fig. 2(d), is 0.29 eV/atom in the In rich limit ($\mu_{\text{In}}=\mu_{\text{In}(\text{bulk})}$). The energy cost is even higher under less In-rich conditions. In the region where the Ga-N dimer surface forms the incorporation of In, as shown in Fig. 2(b), is not favorable. For $\mu_{\text{In}}=\mu_{\text{In}(\text{bulk})}-0.08$ eV it costs 0.33 eV to replace a Ga with an In atom.

As seen in Fig. 2, the larger size of In compared to Ga means that the sp^2 bonding is less effective as a relaxation mechanism if In replaces the Ga on the Ga-N dimer surface. For this reason In incorporation on the Ga-N dimer surface is not favored. However, when In replaces Ga below the indium adlayer, as depicted in Fig. 2(f), the outward relaxation of the In_{Ga} atom leads to a stronger interaction between the adlayer atoms and the In_{Ga} . Thus the presence of the adlayer promotes the incorporation of indium in the underlying layers.

Thus In incorporation is inhibited if hydrogen is too abundant or if the chemical potential of indium is not sufficiently high to stabilize the adlayer. The upper limit on the hydrogen chemical potential depends on the indium chemical potential. In the In-rich limit the upper limit is $\mu_{\text{H}} < \mu_{\text{H}}(T=0) - 0.93$ eV. If the hydrogen chemical potential is greater than this value, then the Ga atoms at the surface will become saturated by H and NH_2 groups, and In incorporation will be inhibited.

Let us now consider In incorporation on the c -plane of the InGaN alloy. The diagram shown in Fig. 3 illustrates regions of $(\mu_{\text{H}}, \mu_{\text{In}})$ phase space in which possible reconstructions are stable. Five structures appear in this diagram. The two

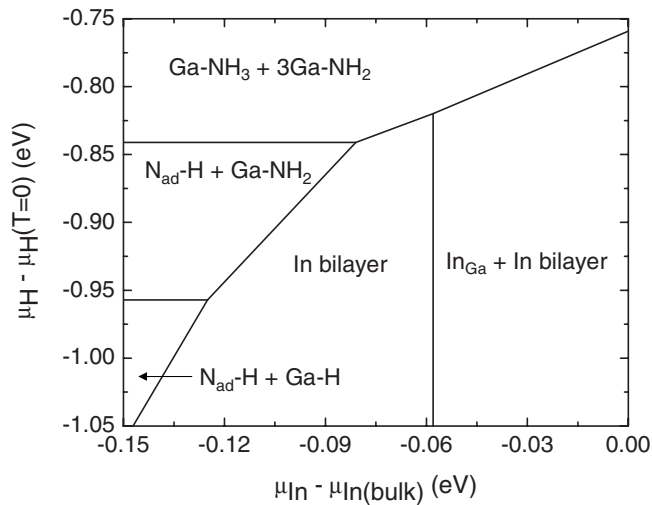


FIG. 3. Results correspond to the *c* plane for a growth temperature of 700 °C. This plot indicates the surface structure that has the lowest energy for various values of the In and H chemical potentials. Endothermic incorporation of indium in surface group-III sites occurs in the region at the lower right labeled $\text{In}_{\text{Ga}} + \text{In bilayer}$. In the other regions In_{Ga} formation is not energetically favorable.

structures that are stable in the lower right section of the diagram are the In bilayer and the $\text{In}_{\text{Ga}} + \text{In bilayer}$. As μ_{In} increases to a value greater than $\mu_{\text{In}(\text{bulk})} - 0.06$ eV it becomes energetically favorable to incorporate In_{Ga} beneath the In layers, and there is a transition between these two structures. The $\text{In}_{\text{Ga}} + \text{In bilayer}$ structure is shown in Fig. 4(a). A high concentration of homogeneously distributed indium is expected if growth takes place under conditions in which this structure is stable.

As seen in Fig. 3, when the hydrogen chemical potential is high the surface is terminated by NH_2 and NH_3 groups. On this surface $\frac{3}{4}$ of the Ga atoms are bonded to a NH_2 and $\frac{1}{4}$ of the Ga atoms are bonded to a NH_3 molecule.¹⁹ Incorporation of In is not favorable on such a surface. The calculations indicate that the energy cost is at least 0.32 eV to incorporate an indium below an NH_3 as shown in Fig. 4(b). Under the H-rich conditions in which this surface is stable, any indium present on the surface will either be desorbed or accumulate in In droplets.

The $\text{N}_{\text{ad}}\text{-H} + \text{Ga-H}$ termination, shown in Fig. 4(c), is stable for low μ_{H} and low μ_{In} . In this growth regime indium incorporation is not exothermic, but the energy cost to incorporate indium below the N adatoms may be quite low. This is seen by comparing the energies of the structures shown in Figs. 4(c) and 4(d). In the $\text{In}_{\text{Ga}} + \text{N}_{\text{ad}}\text{-H} + \text{Ga-H}$ structure one of the three Ga atoms bonded to the N adatom has been replaced by an In atom. For $\mu_{\text{H}} = \mu_{\text{H}}(T=0) - 1.0$ eV and $\mu_{\text{In}} = \mu_{\text{In}(\text{bulk})} - 0.14$ eV the energy cost to form this structure is $\Delta E = 0.06$ eV. This cost is comparable to $k_B T = 0.08$ eV for a growth temperature of 700 °C. Treating the N adatoms as independent one may estimate the number of indium at-

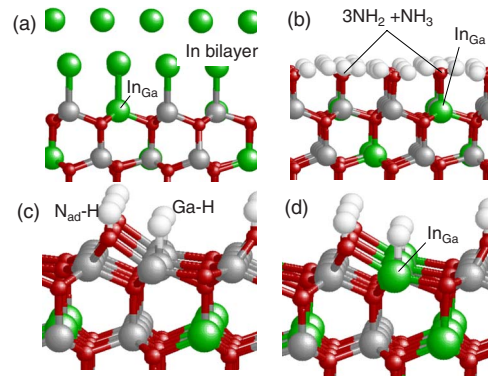


FIG. 4. (Color online) Reconstructions of the InGaN *c*-plane surface are shown. (a) $\text{In}_{\text{Ga}} + \text{In bilayer}$. $\text{In}_{\text{Ga}} + 3\text{NH}_2 + \text{NH}_3$. (c) $\text{N}_{\text{ad}}\text{-H} + \text{Ga-H}$. (d) $\text{In}_{\text{Ga}} + \text{N}_{\text{ad}}\text{-H} + \text{Ga-H}$. In atoms are large green/light gray spheres, Ga atoms are gray, N atoms are small red/gray spheres, and H atoms are white.

oms bonded to each adatom as $f_{\text{In}} = 3 / [\exp(\Delta E / k_B T) + 1]$. The factor of 3 arises because there are three equivalent In_{Ga} sites neighboring each N adatom. For $T = 700$ °C we obtain $f_{\text{In}} = 0.96$. This argument assumes that equilibrium is established in the topmost In/Ga layer—the layer bonded to the N adatoms—and suggests that the number of In atoms in this layer would be approximately the same as the number of N adatoms. Thus a substantial amount of indium may be incorporated in this growth regime. A similar argument holds for the $\text{N}_{\text{ad}}\text{-H} + \text{Ga-NH}_2$ surface.

The preceding analysis indicates that the most important requirement to facilitate incorporation of indium on the *c*-plane is to avoid formation of the $3\text{NH}_2 + \text{NH}_3$ surface. This requirement can be met by limiting the hydrogen chemical potential to a value less than $\mu_{\text{H}} < \mu_{\text{max}} \sim \mu_{\text{H}}(T=0) - 0.85$ eV.

In summary, these calculations indicate that efficient indium incorporation on the *c*-plane and the *m*-plane may be achieved by employing very N-rich conditions, keeping the hydrogen partial pressure below certain limits and increasing the chemical potential of indium to a value that is within about 0.1 eV of the value for which droplets of indium would form. The requirement on the hydrogen abundance appears to be somewhat more stringent in the case of growth on the *m* plane. The results also imply that the surfaces of *m*-plane and *c*-plane InGaN active layers grown by MOCVD may in some cases be covered by indium adlayers immediately following their completion.

The author is grateful to D. Bour, C. Chua, Z. Yang, and N. Johnson for helpful discussions. This research was performed under the DARPA VIGIL Program, managed by Henryk Temkin. The material is based upon work supported by the U.S. Army Research Laboratory and the (U.S.) Army Research Office under Contract No. W911NF-08-C-0003, monitored by John Zavada.

- ¹S. Nakamura, M. Senoh, S. Nagahama, N. Iwasa, T. Yamada, T. Matsushita, H. Kiyoku, and Y. Sugimoto, *Jpn. J. Appl. Phys., Part 2* **35**, L74 (1996).
- ²M. D. McCluskey, L. T. Romano, B. S. Krusor, D. P. Bour, N. M. Johnson, and S. Brennan, *Appl. Phys. Lett.* **72**, 1730 (1998).
- ³Y. Chen, T. Takeuchi, H. Amano, A. Akasaki, N. Yamada, and Y. Kaneko, *Appl. Phys. Lett.* **72**, 710 (1998).
- ⁴I. Ho and G. B. Stringfellow, *Appl. Phys. Lett.* **69**, 2701 (1996).
- ⁵H. Chen, R. M. Feenstra, J. E. Northrup, J. Neugebauer, and D. W. Greve, *MRS Internet J. Nitride Semicond. Res.* **6**, 11 (2001).
- ⁶P. Waltereit, O. Brandt, A. Trampert, H. T. Grahn, J. Menniger, M. Ramsteiner, M. Reiche, and K. H. Ploog, *Nature (London)* **406**, 865 (2000).
- ⁷K. Okamoto, H. Ohta, S. F. Chichibu, J. Ichihara, and H. Takasu, *Jpn. J. Appl. Phys., Part 2* **46**, L187 (2007).
- ⁸M. Ueda, K. Kojima, M. Funato, Y. Kawakami, Y. Narukawa, and T. Mukai, *Appl. Phys. Lett.* **89**, 211907 (2006).
- ⁹A. Chakraborty, T. J. Baker, B. A. Haskell, F. Wu, J. S. Speck, S. P. DenBaars, S. Nakamura, and U. K. Mishra, *Jpn. J. Appl. Phys., Part 2* **44**, L945 (2005).
- ¹⁰F. Schulze, J. Blasing, A. Dadgar, and A. Krost, *Appl. Phys. Lett.* **82**, 4558 (2003).
- ¹¹M. J. Galtrey, R. A. Oliver, M. J. Kappers, C. J. Humphreys, P. H. Clifton, D. Larson, D. W. Saxey, and A. Cerozo, *J. Appl. Phys.* **104**, 013524 (2008).
- ¹²C. K. Gan and D. J. Srolovitz, *Phys. Rev. B* **77**, 205324 (2008).
- ¹³P. Bogusławski, K. Rapcewicz, and J. J. Bernholc, *Phys. Rev. B* **61**, 10820 (2000).
- ¹⁴H. Chen, R. M. Feenstra, J. E. Northrup, T. Zywietz, J. Neugebauer, and D. W. Greve, *J. Vac. Sci. Technol. B* **18**, 2284 (2000).
- ¹⁵H. Chen, R. M. Feenstra, J. E. Northrup, T. Zywietz, and J. Neugebauer, *Phys. Rev. Lett.* **85**, 1902 (2000).
- ¹⁶E. L. Piner, M. K. Behbehani, N. E. El-Masry, F. G. McIntosh, J. C. Roberts, K. S. Boutros, and S. M. Bedair, *Appl. Phys. Lett.* **70**, 461 (1997).
- ¹⁷A. Sohmer, J. Off, H. Bolay, V. Harle, V. Syganow, J. S. Im, V. Wagner, F. Adler, A. Hangleiter, A. Dornen, F. Scholz, D. Brunner, O. Ambacher, and H. Lakner, *MRS Internet J. Nitride Semicond. Res.* **2**, 14 (1997).
- ¹⁸J. E. Northrup, R. Di Felice, and J. Neugebauer, *Phys. Rev. B* **56**, R4325 (1997).
- ¹⁹C. G. Van de Walle and J. Neugebauer, *Phys. Rev. Lett.* **88**, 066103 (2002).
- ²⁰J. E. Northrup and C. G. Van de Walle, *Appl. Phys. Lett.* **84**, 4322 (2004).
- ²¹The energy of the $\text{In}_{0.25}\text{Ga}_{0.75}\text{N}$ alloy is calculated using a cell containing six Ga, two In, and eight N atoms. The cell dimensions and internal coordinates are fully relaxed. InGaN alloys with this indium concentration are known to be metastable: according to the present work the separation of In and Ga into fully relaxed InN and GaN would lower the energy by ~ 0.04 eV per N atom. Such phase separation is inhibited by kinetics for realistic growth temperatures.
- ²²W. Kohn and L. J. Sham, *Phys. Rev.* **140**, A1133 (1965).
- ²³R. Stumpf and M. Scheffler, *Comput. Phys. Commun.* **79**, 447 (1994).
- ²⁴D. M. Ceperley and B. J. Alder, *Phys. Rev. Lett.* **45**, 566 (1980).
- ²⁵N. Troullier and J. L. Martins, *Phys. Rev. B* **43**, 1993 (1991).
- ²⁶H. Monkhorst and J. Pack, *Phys. Rev. B* **13**, 5188 (1976).